Influence of Substrate Bias Voltage on Corrosion and Wear Behavior of Physical Vapor Deposition CrN Coatings

Khalil Aouadi, Brahim Tlili, Corinne Nouveau, Aurélien Besnard, Moez Chafra, and Rania Souli

The objective of the present paper is to study the influence of the substrate bias voltage on the microstructure, composition, deposition rate, tribological and corrosion properties of CrN coatings obtained by DC magnetron sputtering on 90CrMoV8 steel and Si (100) substrates. The substrate bias voltage varied from 0 to − 700 V. The deposited films were characterized by SEM, XRD and potentiodynamic polarization. The wear behavior and coefficient of friction were determined and investigated after rotative tribometer tests. The results indicated that the substrate bias voltage considerably affected the intrinsic properties of the CrN films. Indeed, it significantly influenced the grain size and the root-mean-squared roughness which varied from 20 to 29 nm, and from 9 to 19 nm, respectively, when polarization changed from 0 to − 700 V. All the CrN coatings have a dense columnar structure and are well crystallized according to the XRD analyses. Nevertheless, it has been shown that the peaks intensity decreased by increasing the substrate bias voltage. By applying a substrate bias voltage, it was obvious that the friction behavior was enhanced, and the wear volume was decreased. Finally, the CrN coating obtained under a substrate bias voltage of − 500 V presented the best corrosion resistance and wear resistance probably due to its dense microstructure.

Keywords corrosion, CrN coatings, substrate bias voltage, tribology, wear

1. Introduction

Binary CrN layers developed by PVD methods are well studied for many years. Generally, during machining process, several interactions in the cutting zone occur. Therefore, these interactions (such as vibration, friction, plastic and elastic deformation.) can be the cause of different types of cutting tools damages (Ref 1). That is why it is necessary to improve the properties of cutting tools. This issue was the subject of several previous studies (Ref 2, 3) in which PVD thin films on the cutting tool surface were an efficient solution.

Chromium nitride (CrN) is widely known as a protective coating in cutting tool material. It is characterized by a good tribological behavior, a good wear and corrosion resistance and a high oxidation resistance. To improve this coating, several studies were performed using different parameters and various conditions: Polcar et al. (Ref 4) developed CrN coatings under different deposition temperatures by low arc deposition technology. They showed that the tribological behavior of the CrN layers strongly depends on the temperature. In fact, when increasing temperature from 25 to 500 °C, the friction coefficient of a CrN layer against a Si_3N_4 ball decreases whereas when sliding against an Al_2O_3 ball, the lowest friction of coefficient is obtained at 25 and 500 °C.

Inoue et al. (Ref 5) developed CrN coatings by RF reactive sputtering. They studied the pressure of nitrogen (P_{N2}) variation in the vacuum chamber. They observed an influence on the nitrogen chemical composition, crystal structure, internal stresses of the CrN layers and showed that lower was the nitrogen pressure, better were the mechanical properties of the CrN films. Other works have chosen to study the effect of the process on the properties of the CrN coatings such as Hurkmans et al. (Ref 6) who developed CrN coatings by unbalanced magnetron sputtering (UBM) and arc/unbalanced magnetron arc sputtering (ABS) spray techniques. Lin et al. (Ref 7) compared the properties of CrN coatings developed by DC magnetron sputtering (DCMS), pulse magnetron sputtering (PMS) and magnetron sputtering technique pulsed power (MPP). Other studies deal with CrN coatings obtained with high pulsed power magnetron sputtering (HPPMS) (Ref 8). Then, magnetron sputtering (MS) is the most commonly used technique to synthesize CrN films (Ref 9, 10). Other previous studies showed the influence of the substrate on the CrN layers properties. Nouveau et al. (Ref 11) developed CrN coatings on carbide substrates. They exhibited that the substrate had a main impact on the adhesion of the coating and influenced its tribological behavior. The substrate bias voltage remains an essential parameter which affects the mechanical, tribological and structural properties of PVD coatings. This parameter acts directly on improving the atoms mobility and has an influence on

Khalil Aouadi, Arts et Metiers ParisTech, LaBoMaP, Rue Porte de Paris, 71250 Cluny, France; and Laboratoire de recherche Structures et Mécanique APpliquée (LASMAP), Ecole Polytechnique de Tunisie, Université de Carthage, La Marsa, Tunisia; **Brahim Tlili** and **Rania Souli**, Ecole Nationale d'Ingénieurs de Tunis, Laboratoire de Mécanique Appliquée et Ingénierie (LR-MAI), Université de Tunis El-Manar, 1002 Tunis, EL Manar, Tunisia; **Corinne Nouveau** and **Aurélien Besnard**, Arts et Metiers ParisTech, LaBoMaP, Rue Porte de Paris, 71250 Cluny, France; and **Moez Chafra**, Laboratoire de recherche Structures et Mécanique APpliquée (LASMAP), Ecole Polytechnique de Tunisie, Université de Carthage, La Marsa, Tunisia. Contact e-mail: aouadikhalil@hotmail.com.

the effect of the coating's ion bombardment (Ref 12). Oden et al. (Ref 12) developed CrN coatings using different negative substrate bias voltage which varied between 20 and 400 V by arc evaporation. They confirm that increase in the substrate bias voltage causes an increase in lattice defect density and an increase in compressive residual stress and a decrease in column width when the bias increase from − 20 to − 100 V. Also, the hardness enhances and the critical load decreases when the bias is between − 20 and − 100 V. Wang et al. (Ref 13) deposited CrN films by arc ion plating, and they change the bias voltage between 0 and − 400 V. They confirm that the increase in bias voltage induced a change of CrN preferred orientations from (200) to (220). Also, there is a slight effect on chemical composition of the coatings and the deposition rate increases. Warcholinski and Gilewicz (Ref 14) developed CrN coatings by cathodic arc evaporation technique. They studied the effect of substrate bias voltage on the properties of CrN coatings. They confirm that compressive residual stress increases from 1 to 2.1 GPa when the bias voltage increases from − 10 to − 70 V. Beyond of − 70 V, compressive residual stress decreases. Also, the application of bias voltage improves the hardness of CrN coating and the maximum value is shown at − 150 V. Valleti et al. (Ref 15) developed CrN coatings by cylindrical cathodic arc deposition. They studied the influence of bias voltage on the properties of CrN films. They verified that columnar grain size decreases with the increase in bias voltage. Also, mechanical properties decrease with the increase in bias voltage. The application of bias voltage improves the corrosion resistance. Luo et al. (Ref 16) deposited CrN coating by magnetron sputtering, and they studied the effect of substrate bias voltage. They varied the bias voltage between 0 and − 150 V. They observe that preferred orientation CrN coatings changes when bias voltage arises and the film deposited at − 100 V showed the best mechanical properties. Kong et al. (Ref 17) deposited a CrN films by medium-frequency magnetron sputtering. They varied the negative substrate bias voltage between − 100 and − 500 V. They observed that below − 300 V, the surface roughness decreases and the nitrogen concentration increases. Also, they observed the generation of a tensile stress. Above − 300 V, the texture of CrN changes from (111) to (200). Meanwhile, a compressive stress is generated. They confirmed that the grain size decreases with the increase in bias voltage and the deposition rate decreases.

Thus, it can affect the chemical composition of coatings, the deposition rate (Ref 18), the preferred orientation of the CrN layers, their mechanical properties (Ref 19, 20) and their adhesion strength and residual stresses (Ref 21).

In the present work, we used an industrial machine (KENOSISTEC-KS40V) to deposit CrN coatings under various substrate bias voltage (0, − 200, − 300, − 500, − 600 and − 700 V) by reactive DC magnetron sputtering. The deposition rate, chemical composition, grain size, microstructure, friction, wear and corrosion resistance were investigated as a function of the substrate bias voltage.

2. Experimental

2.1 Substrates

CrN films were deposited on stainless steel (90CrMoV8) samples (20 × 20 mm^2 and 5 mm thick) with a surface roughness R_a of 0.5 µm and mirror-polished silicon (100) which have an area of 10 × 10 mm and a thickness of ∼ 380 µm. Before deposition, all the substrates were ultrasonically cleaned in acetone and ethanol for 5 min each and then dried under compressed air.

2.2 Coatings

The CrN coatings were deposited by DC reactive magnetron sputtering (KENOSISTEC-KS40V).

Before deposition, all substrates were in situ etched under an argon plasma at − 700 V for 10 min to ensure a better adhesion of the coatings. The substrate temperature during applying substrate bias voltage of − 700 V is about 400 °C which is below tempering of the steel substrate. Prior deposition, the chamber was evacuated to a pressure lower than 2 × 10^{-5} Pa and heated at 300 °C for 7 h. During deposition, the working pressure was set at 0.5 Pa. The flow rates of Ar and N_2 were 68.8 and 33.3 sccm, respectively. A chromium target with purity of 99.95% and (406.4 × 127) mm^2 dimensions was used for the deposition process. The Cr target power was set at 1500 W (− 375 V). To study the effect of the substrate bias voltage on the properties of the CrN films, different voltages were applied from − 200 to − 700 V. The deposition time was fixed at 2 h. Table 1 summarizes the CrN deposition conditions.

2.3 Characterizations

The surface morphology and the microstructure of the coatings were observed by SEM field emission (JEOL JSM 7610F). The chemical composition of the wear track after tribometer tests of CrN films was determined by EDS and WDS analysis (JEOL JSM 6400F). The structure of CrN films was studied by XRD (INEL diffractometer type curve CPS 120 detector, K_α Co radiation source of 0.178897 nm) with a voltage of 25 kV and a current of 25 mA. The crystallite size of CrN films was calculated using Scherrer's formula. Rotative ball-on-disk tests under a fixed load of 2 N, a sliding speed of 3 cm/s and a sliding distance of 200 m, using an alumina ball (Al_2O_3) 6 mm of diameter as the counterpart permitted to determine the friction coefficient, while the wear volume of the CrN layers was estimated from 3D optical profilometer (VEECO, Wyko-NT 1100) profiles. The wear volume was calculated from profilometer profiles. To be more precise, we chose eight sections of depth in the wear track. The film surfaces topography was analyzed by atomic force microscope (AFM) (type XE Park 70) using the tapping mode. We chose to scan an image with (5 × 5) $µm^2$ dimensions. Additional analyses with the Gwyddion software were performed to determine the RMS roughness of the CrN coatings; this method has been used by other works (Ref 17, 21). The residual

Table 1 Deposition conditions of the CrN coatings

Argon flow rate, sccm	68.8
Nitrogen flow rate, sccm	33.3
Working pressure, Pa	0.5
Deposition time, h	2
Temperature, °C	300
Substrate bias voltage, V	0, − 200, − 300, − 500, − 600, − 700
Power of the Cr target, W	1500
Target bias voltage, V	− 375

stresses were determined using the Stoney's formula (Ref 22) (Eq 1).

$$\sigma = \frac{E_S}{6(1-\nu_S)}\frac{e_S^2}{e_f}\left(\frac{1}{R}-\frac{1}{R_0}\right) \quad \text{(Eq 1)}$$

where E_s: Young's modulus of the substrate, ν_s: Poisson's ratio of the substrate, e_s: substrate thickness, e_f: film thickness, R: radius of curvature after deposition and R_0: radius of curvature before deposition. The radius of curvature before and after deposition is determined using a 3D optical profilometer (VEECO, Wyko-NT 1100) and the Gwyddion software. The hardness of CrN coatings has been measured by means of nanoindentation tests using a MTS XP Nanoindenter equipped with a Vickers indenter. The maximum load is about 750 mN, and the indentation depth is about 1.7 µm. The hardness is calculated using the Rahmoun's model (Ref 23). Thereby, according to this model, to evaluate the hardness of the coating, it is necessary that the indentation depth must be superior to the thickness of the coating. This model permits us to calculate the hardness and Young modulus of coating without the effect of substrate. The adhesion tests were carried out by means of a micro-scratch tester (Scratch Tester Millennium 200) equipped with Rockwell spherical diamond indenter and fitted with an acoustic emission detector. For each sample, an average adhesion value is calculated from three to five tests. The electrochemical measurements were conducted in a conventional three-electrode electrolytic cell (volume of 200 mL) under free air condition. To simulate a corrosive environment containing Cl^- ions, an aqueous solution of 3 wt.% NaCl was used. The polarization curves were obtained while potential was scanned in the interval [$E_{ocp} \pm 250$ mV].

3. Results and Discussion

3.1 Chemical Composition and Residual Stresses

The chemical composition and residual stresses of the CrN layers are summarized in Table 2.

The influence of the substrate bias voltage on the chemical composition is shown in Fig. 1. All the CrN films contain Cr, N and a small amount of O. The results showed that the chemical composition of the CrN coatings varies slightly with the substrate bias voltage. By applying a bias voltage of − 200 V, the N content increases from 44 to 46 at.% while the Cr content decreases from 52 to 49 at.%. Therefore, the N/Cr ratio increases from 0.84 to 0.93. This can be explained by the increase in the ion bombardment energy that increases with the substrate bias voltage. This energy is transferred to the atoms. So, its mobility increases (Ref 24). This phenomenon can be considered as a local annealing called "thermal spike" (Ref 25). Consequently, the imprisoned atoms get more energy and move to the interstitial sites. With the increase in the bias voltage, the chemical composition of Cr varied between 46 and 50 at.%. Also, a slight variation of the nitrogen composition is observed, and it varies between 45 and 49 at.% by increasing the voltage from − 200 to − 700 V. However, the N/Cr ratio was not very influenced by the variation of the substrate bias voltage and varies from 0.9 to 1. This is confirmed by previous studies (Ref 17, 25). Ovcharenko et al. (Ref 24) studied CrN coatings obtained with a substrate bias voltage from − 70 to − 300 V. They observed an increase in the Cr/N ratio from 0.95 to 1.

Figure 2 represents the residual stresses and grain size as a function of the substrate bias voltage. By applying a substrate bias voltage between 0 and − 200 V, the residual stresses are compressive while they are tensile when increasing the bias voltage to − 300 V. It is known that the residual stresses come from intrinsic and thermal stresses. For the lowest substrates bias voltage (− 200 V), we observe that the residual stresses are very low (− 10.5 MPa). This can be assigned to the surface roughness. Indeed, when the surface is rough enough, it promotes the formation of tensile stresses due to the simplicity of contact between the neighboring grains (Ref 26). By increasing the substrate bias voltage from − 300 to − 500 V, the tensile stresses also increase because the incident ion energy

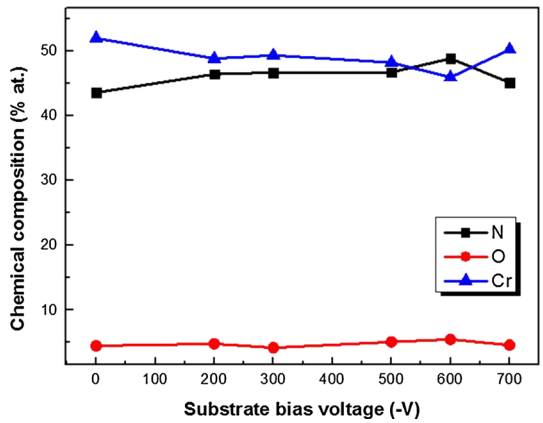

Fig. 1 Chemical compositions of CrN films as a function of the substrate bias voltage

Table 2 Chemical composition, thickness, grain size, RMS roughness and residual stresses of CrN coatings as a function of the substrate bias voltage

Bias voltage, V	Thickness, µm	Composition, at.%				RMS, nm	Residual stresses, MPa
		Cr	N	O	N/Cr		
0	1	52	44	4	0.84	18.8	0
− 200	1.14	49	46	5	0.93	17.8	− 10.5
− 300	1.09	49	47	4	0.95	13.56	63.1
− 500	0.87	48	46	5	0.95	11.02	86.4
− 600	1.07	46	49	5	1.06	8.98	21.7
− 700	1.05	50	45	5	0.9	12.43	− 100.5

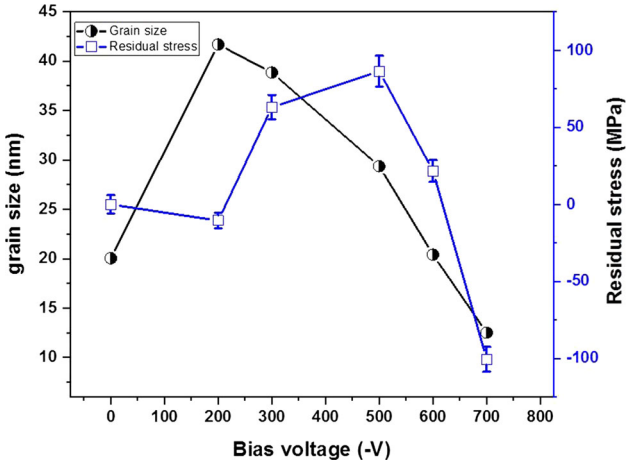

Fig. 2 Residual stresses and grain size of the CrN films as a function of the substrate bias voltage

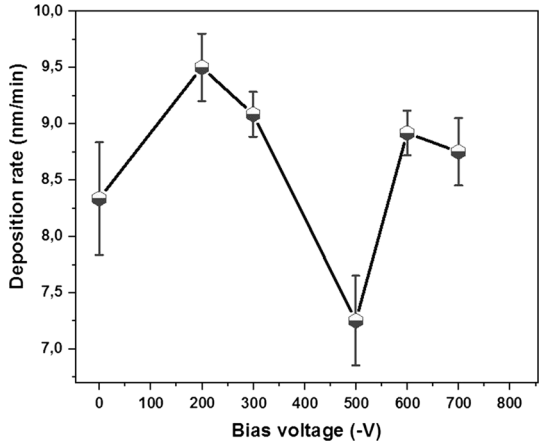

Fig. 3 Evolution of the deposition rate and grain size of CrN film as a function of the substrate bias voltage

that arrives on the substrate will increase its temperature (Ref 27). Thus, the thermal stresses are dominant. This phenomenon will increase the T_s/T_m ratio (T_s is the substrate temperature and T_m is the melting temperature of the coating) and will lead to an inhomogeneous temperature distribution between the substrate and the films. The consequence is the increase in the residual stresses of the CrN films. When the substrate bias voltage increases from − 500 to − 700 V, we observe that the tensile stresses change and become compressive. Similar results are observed by Kong et al. (Ref 17). This state of stresses change is probably due to the increase in the substrate bias voltage which causes an increase in the ion energy. While arriving at the substrate surface, the atoms etch the film, penetrate, will be trapped and lead to film growth defects (Ref 25, 28). Typically, compressive residual stresses arise when the film is bombarded during its growth under ions with an energy from ten to hundreds eV. In this case, several defects occur such as stacks, low-angle grain, which causes the deformation of the lattice parameter. According to Wang et al. (Ref 28), residual stresses can be relaxed by thermal spikes, resulting in the release of the strain generated by the contact between atoms and substrate. Therefore, residual stresses in the films will decrease at high substrate bias voltage such as − 700 V. Likewise, we observe that all coating present a small value of stress. Residual stress in PVD coatings mainly generates from the contribution of intrinsic stresses and thermal stresses. In our case, the evolution of the residual stresses is dominated by the thermal stresses. In general, in the case of the elaboration of CrN films without heating substrate, residual stresses are compressive and their values are in the order of GPa (Ref 7, 14). In our case, the thermal stresses are dominant which arises a strong relaxation of stresses, because of this, the stresses are very small.

The evolution of the grain size as a function of the substrate bias voltage is shown in Fig. 2. The grain size increases with the application of a bias voltage of − 200 V from 20.05 to 41.68 nm. This increase in grain size is the result of the high mobility of adatoms due to the high-energy ions that promote the migration of particles at grain boundaries and therefore increases the size of the grains (Ref 29). Chang et al. (Ref 20) explained this increase by the increase in the impinging ions with the increasing of bias voltage which increases the defect density and disturbs the growth of grains. Consequently, the gain in energy per atom and the destabilizing effect of bombardment increase with the increase in bias. By increasing bias voltage to − 700 V, grain size decreases until 12 nm. It is well known that defects in the film prohibit the migration of particles to grain boundaries. Furthermore, the increased number of surface defects is responsible for more preferential nucleation sites, which may cause a decrease in the grain size (Ref 30).

3.2 Microstructure and Morphology

The substrate bias voltage has an influence on the deposition rate as shown in Fig. 3. We observed that the deposition rate ranges from 7.25 to 9.5 nm min^{-1} when the substrate bias voltage increases from 0 to − 700 V. The highest deposition rate is obtained at a bias voltage of − 200 V. This can be explained by the increase in the flux and energy of the ion bombardment of the substrate surface (Ref 31). Ma et al. (Ref 32) explained the increase in the deposition rate during the deposition to the Ar^+ cations and clusters of the sputtered material in the plasma which are attracted by the low substrate voltage. This leads to a higher deposition rate. Then, it drops from 9.5 to 7.25 nm min^{-1} when the bias voltage increases from − 200 to − 500 V. This decrease is due to the risen temperature. The increase in substrate bias voltage induces an increase in substrate temperature. The etching rate increases with the increasing temperature. Thus, the deposition rate decreases (Ref 32). It is well known that positives ions are attracted by the substrate negatively polarized and transfer their kinetic energy to the atoms at the surface of the biased substrate (Ref 33). Then, the energy of the incident ions becomes higher when the bias voltage of the substrate increases. Consequently, several atoms of the surface are re-sputtered (Ref 25). Moreover, this decrease in the deposition rate could be explained by the decrease in the energy of the atoms arriving on the substrate because of a large amount of collisions. For a bias voltage of − 500 V, we note that the deposition rate is the lowest one. When we increase the substrate bias voltage to − 600 and − 700 V, we note that the deposition rate increases again. This phenomenon may be due to the effect of higher substrate bias voltage which can produce a great attraction in drawing the metallic ions (Ref 29). So, the deposition rate increases.

The cross sections of the CrN layers were observed by SEM. Figure 4 shows the microstructure of the CrN films obtained with a substrate bias voltage of 0, − 200, − 300, − 500, − 600 and − 700 V. The SEM images showed that the CrN

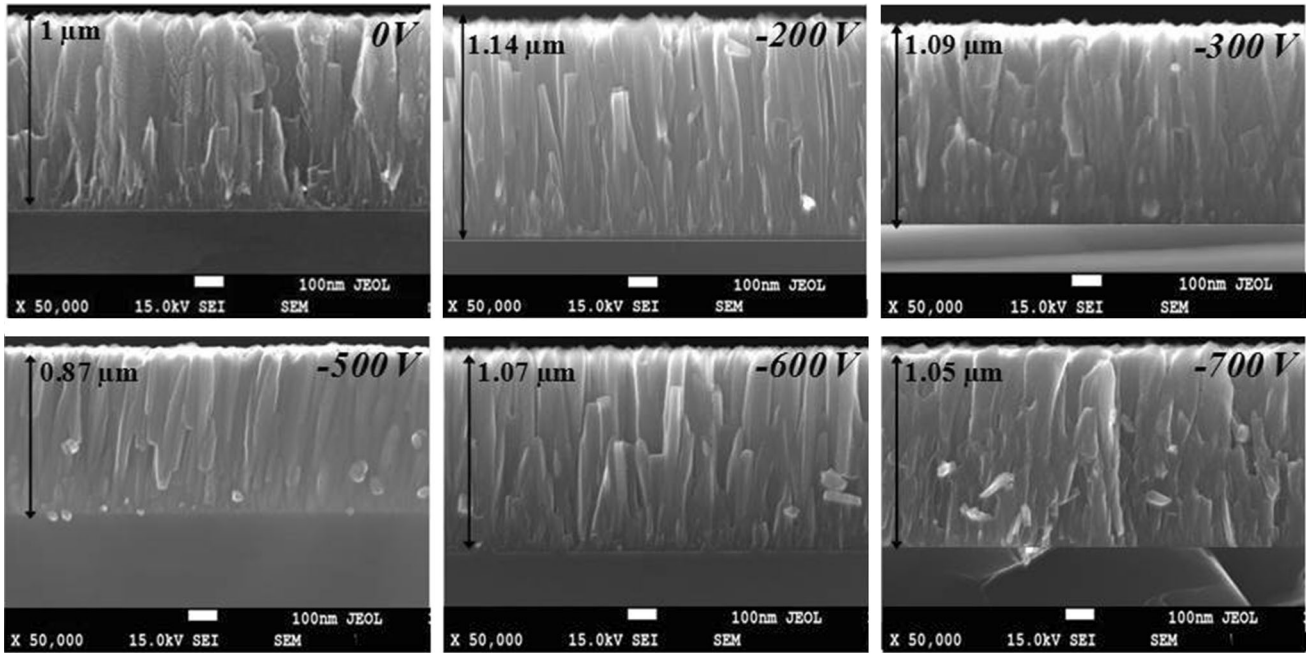

Fig. 4 Cross-sectional SEM images of the CrN coatings as a function of the substrate bias voltage

coatings present a columnar and dense microstructure. The films thicknesses vary between 0.87 and 1.14 µm. A comparison of thicknesses shows a slight decrease when the bias value is about − 500 V where the thickness is 0.87 µm. One possible cause of this phenomenon could be explained by the considerable impact on the metal ions to a high enough bias voltage of the substrate, which can reduce the deposition rate (Ref 29). When the substrate bias voltage increases from − 200 to − 700 V, the structure becomes denser and the vacant sites are reduced. This is due to the high mobility of the adatoms induced by the high-energy of the ion bombardment leading to the migration of small grains to grain boundaries and as a consequence, to higher grain size (Ref 21). At high temperatures, the mobility of the adatoms increases. Then, they can fill the voids between the grains and break the strong growth of the columns which increases the density of the coatings (Ref 34).

The substrate bias voltage also affected the surface morphology of CrN films as confirmed by the three-dimensional topographic AFM images in Fig. 5. Indeed, we can notice that the grain size of the coating obtained for a substrate bias voltage of − 200 V are the highest ones while the CrN film obtained at − 700 V presents the smallest ones. That confirms our previous results (Fig. 2). The surfaces are globally uniform and composed of domes and craters. Dimensional measurements showed that the domes had a mean diameter of about 150 nm and that the craters had a maximum depth of 50 nm. In addition, Fig. 5 shows the RMS roughness as a function of the substrate bias voltage. We verified by AFM that the CrN layer obtained with a substrate bias voltage of 0 and − 200 V presents the highest RMS which can confirm our hypothesis on the residual stresses level of this coating (Fig. 2). Besides, the RMS roughness decreases from 18.8 to 8.98 nm while the substrate bias voltage increases from 0 to − 600 V. Similar results were observed in the literature (Ref 34, 35). Tsai et al. (Ref 25) showed that the roughness of (TiVCrZrHf)N films obtained by reactive radio-frequency (RF) magnetron sputtering decreases from 23.1 without substrate polarization to 0.8 nm with a substrate bias voltage of − 200 V. They explained this result by the increase in the ions flux and energy that conduced to atomic mobility and densification of the coating (Ref 25). Furthermore, this decrease in the roughness can be also due to the reduction of surface defects (Ref 24). Moreover, densification of the structure and grain refinement can be attributed to the reduction of surface roughness (Ref 36). Also, the increase in bias voltage leads to a high mobility of the adatoms and nucleation density. In addition, under high-energy ion bombardment, highly mobile adatoms can be diffused into the inter-grain voids and the film becomes more compact and denser (Ref 36). Finally, for a substrate bias voltage of − 700 V, an increase in roughness is observed up to 12.43 nm. This can be caused by high-energy bombardment (Ref 21).

The XRD patterns of the obtained CrN films as a function of the substrate bias voltage are shown in Fig. 6. The CrN film obtained without substrate polarization (0 V) presents a characteristic CrN (111) diffraction peak of the fcc cubic structure at 44.6° (ICDD 96-901-1575). A minor CrN (200) diffraction peak at 52.01° is also detected. We can observe that the CrN (111) diffraction peak is slightly shifted to a greater diffraction angle; this is justified by the residual stresses results (Fig. 2). Indeed, the theoretical angle is 43.8°. As expected, the CrN layer obtained with a substrate bias voltage (− 200 V) is very well crystallized with a major CrN (111) diffraction peak detected at 44.1° due to it important grain size. A minor CrN (311) diffraction peak is also detected at 91.9°. The disappearance of the CrN (200) orientation can be caused by a decrease in the strain energy which corresponds to a variation of the residual stresses (Ref 37). Besides, the substrate bias voltage causes a significant increase in the CrN (111) peak intensity. This can be explained by the increase in the grain size (Fig. 2). For a substrate bias voltage of − 300 V, the CrN (111) major diffraction peak is still detected at 43.9° but with a lower intensity. This may be due to the lower rate deposition and smaller grain size (Ref 32). A minor CrN (311) diffraction peak at 91.29° is also detected. The coating obtained at − 500 V

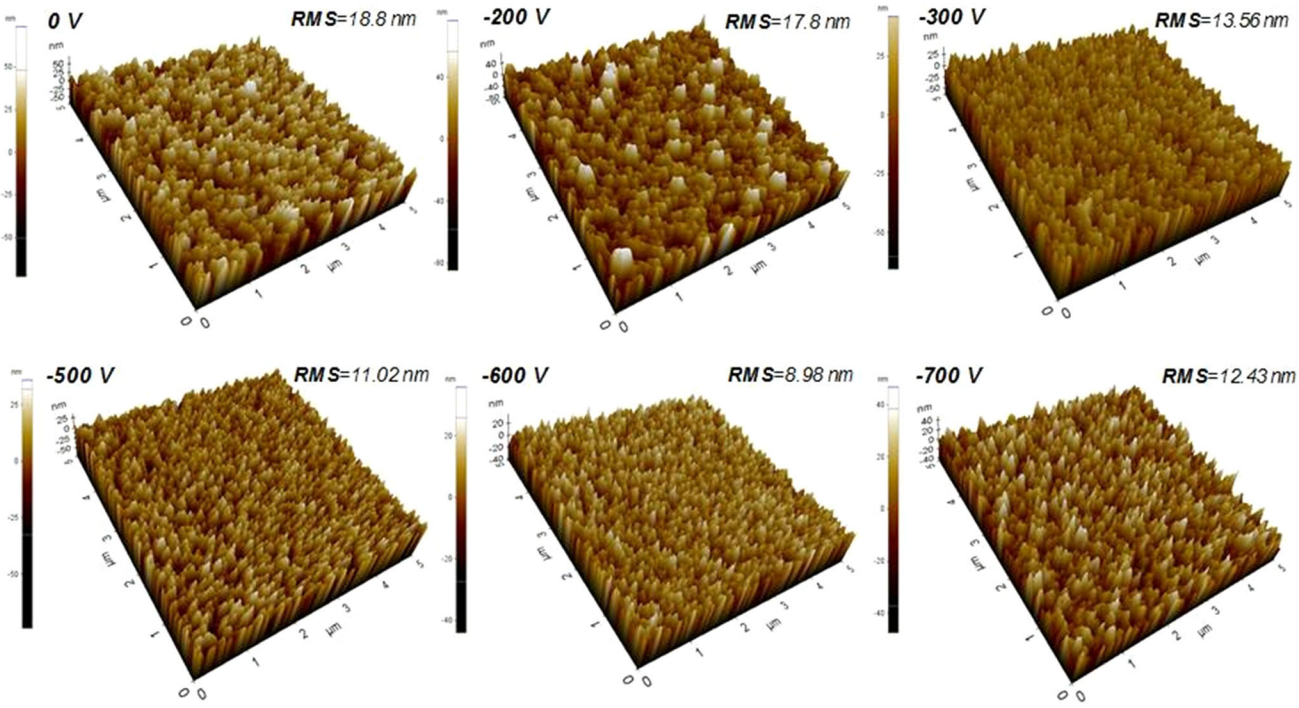

Fig. 5 Three-dimensional topographic AFM images and RMS roughness of CrN coatings as a function of the substrate bias voltage

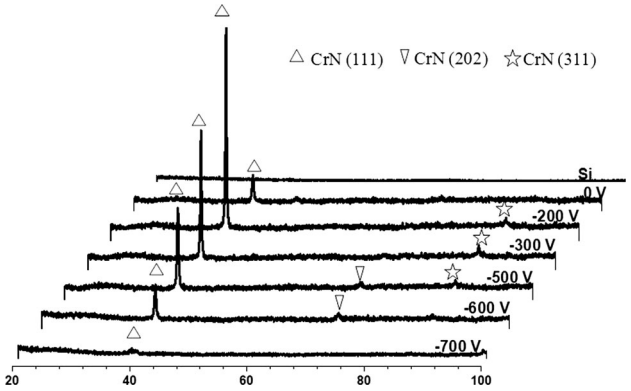

Fig. 6 XRD patterns of CrN films as a function of the substrate bias voltage

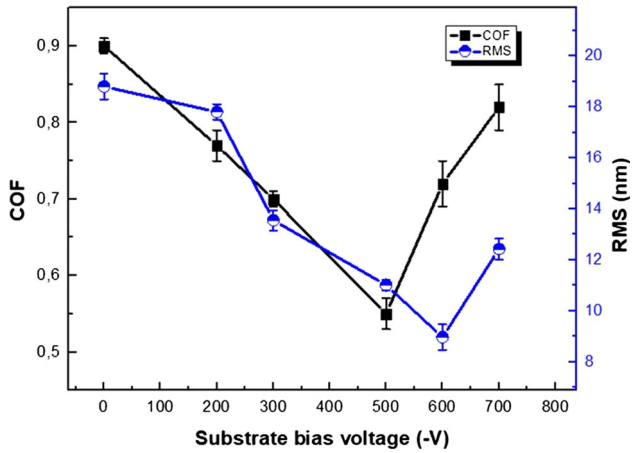

Fig. 7 Coefficient of friction and RMS roughness of the CrN coatings as a function of the substrate bias voltage

presents the CrN (111) at 43.73° but with a lower intensity, a minor CrN (311) at 91.17° as the appearance of a minor CrN (202) at 75.2° (theoretical angle of 75.38°). Similar results were observed by Oden et al. (Ref 12) who studied CrN films obtained by arc evaporation with different substrate bias voltages. At − 600 V, the CrN (311) diffraction peak disappeared while a low intense CrN (111) at 43.79° diffraction peak coexisted with a more intense CrN (202) at 75.23° diffraction peak. Finally, the coating obtained at − 700 V only presents a minor CrN (111) diffraction peak at 43.63°. Then, all our CrN films present the CrN (111) preferred orientation. According to Pelleg et al. (Ref 38) this is due to the dominance of the strain energy during the films growth. Indeed, a change of a thin film texture is related to its free energy minimization. This energy is composed of the surface energy and the strain energy. In the case of nitrides, if the surface energy dominates, the preferred orientation is (200). However, if the strain energy dominates, the preferred orientation is (111). Likewise, Wang et al. (Ref 36) showed that cubic structure of metals is mainly composed of (111) plans and has the lowest surface energy. In addition, the intensity of the CrN (111) diffraction peak decreases while the substrate bias voltage increases. This can be due to the reduction of grain size (Fig. 2). Also, this peak is shifted to higher 2θ which is attributed to the stress reduction in the coating. Likewise, this may be due to the lattice expansion (Ref 38) and to the lattice defects caused by a high energetic ion bombardment (Ref 35).

3.3 Tribological Properties

3.3.1 Coefficient of Friction. Figure 7 shows the RMS roughness and the coefficient of friction (COF) of the CrN films after sliding against Al_2O_3 balls (normal load of 2 N) as a

function of the substrate bias voltage. The COF curve fits very well with the RMS one. This confirms the relation between these two parameters. The COF was determined from the stabilized zone. We mentioned that the friction coefficient of the 90CrMoV8 steel is about 0.98. For the CrN films deposited without substrate polarization (0 V), the COF is about 0.9. With a substrate polarization, the COF of the CrN films varied between 0.5 and 0.8 and it is lower than those obtained without substrate polarization. Thus, the variation of the substrate bias voltage has main effect on the COF. Similar results have been shown in several other studies (Ref 32, 39). Figure 7 shows that the COF decreases from 0.9 to 0.55 when the substrate bias voltage increases up to − 500 V. As expected, this decrease in the COF can be attributed to the decrease in the surface roughness of the CrN films (Fig. 7). Zhou et al. (Ref 40) showed that the COF of CrN coatings varies from 0.5 to 0.65 according to the deposition conditions and the normal load applied during the ball-on-disk test. For the highest substrate bias voltage of − 700 V, the COF increases near 0.8. In contrast, the CrN film roughness obtained at − 600 V is lower than that obtained at − 500 V while its COF is higher. This result can be explained by a better surface morphology and lower defects on the surface of the coating obtained at − 600 V (Ref 34).

3.3.2 Wear Rate. The wear volume was calculated after the ball-on-disk tests. Figure 8 shows the wear rate and the COF of the different CrN films studied. It is noteworthy that the CrN coating obtained without substrate polarization has the highest wear rate. Then, one can conclude that the application of a polarization to the substrate improves the wear behavior of the CrN layers. With a substrate polarization, it is obvious that the wear rates are higher for CrN films obtained at − 200, − 600 and − 700 V than those obtained at − 300 and − 500 V. Moreover, the wear rate at − 300 and − 500 V are very similar. For the coating obtained at − 200 V, one can notice that it has a higher COF than the coatings realized at − 300 and − 500 V. Then, we can conclude that higher the COF is, greater the wear rate is (Fig. 8). This has been also shown by Kok et al. (Ref 41). Besides, the wear rate depends on the substrate bias voltage. This has been proved by Romero et al. (Ref 42) who have shown that the wear rate decreases when the substrate bias voltage increases.

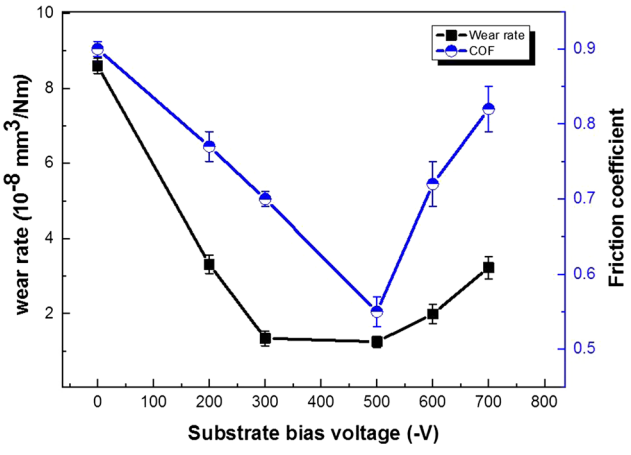

Fig. 8 Wear rate and COF of CrN coatings as a function of the substrate bias voltage

3.3.3 Wear Track Analyses. The wear tracks of the CrN films were observed by SEM and analyzed by EDS. Thereby, the maps of the chemical elements present in the wear tracks were determined (Fig. 9). Generally, after wear tests a significant amount of oxide occurs, which indicates the existence of a local temperature in the contact area between the ball and the surface. The wear track of the CrN film obtained without substrate polarization reveals the presence of debris. Iron and molybdenum, which come from the substrate, and few oxygen traces also exist. This proves the removal of the CrN coating and the oxidation of the substrate. For the CrN film obtained at − 200 V, the same result is observed. For a substrate bias voltage of − 300 V, chromium and nitrogen are detected as a small amount of iron and oxygen. A similar result is obtained for the CrN film deposited at − 500 V. This proves the existence of CrN after the friction test. These results confirm the above ones about the wear rate (Fig. 8). We can note that the amount of iron for the CrN film obtained at − 500 V is lower than that of the CrN film obtained at − 300 V. Moreover, when the substrate bias voltage reached − 600 V, iron and molybdenum are again detected. Therefore, the layer of CrN disappeared after the friction test. For a substrate bias voltage of − 700 V, there is a total disappearance of the CrN layer and only iron is detected. Even if this layer has a lower wear rate than the CrN layer obtained without substrate polarization, we observed a complete removal of the coating in both cases. This is concluded from the SEM image chemical elements profiles of the wear track (Fig. 9). The debris observed in the case of the coating obtained without substrate polarization could explain its higher wear rate.

3.4 Mechanical Properties

The hardness and Young modulus of the CrN films as a function of the substrate bias voltage are listed in Table 3. One can note that the hardness curve fits well with the Young modulus one. The hardness and Young modulus increase and reach a maximum of 22 and 244 GPa, respectively, for a substrate bias voltage of − 500 V. For higher substrate polarization, these two parameters decrease to a minimum of 15 and 211 GPa, respectively. Generally, film hardness is affected by various parameters such as microstructure, grain size, internal stresses. The CrN film obtained without substrate polarization has the lowest hardness. This may be due to its porous structure (Fig. 4). When the substrate bias voltage increases from 0 to − 500 V, the hardness and elastic modulus increase too. This is probably due to the grain size effect (Ref 32) (Fig. 2). In fact, the grain boundary hinders the dislocation movement and the resulting slip because of the discontinuity from a grain to another and the various orientations of grains. So, when the grain size is small, the density is high and the effect of dislocation blocking increases (Ref 27). Also, this increase in hardness can be explained by the ion bombardment effect (Ref 20). Biswas et al. (Ref 43) explained this increase to the increase in the bombarding energy which rises with the increase in the bias voltage. As a result, the adhesion between coating and substrate within the columns. Thereby, hardness of coatings increases. Likewise, the structure densification process can improve hardness (Ref 44). In fact, when the microstructure becomes denser, defects in coatings were effectively reduced. This is confirmed by Fig. 5. Also, Bait at al (Ref 45) related the higher value of hardness to the roughness. This can explain the good hardness of films deposited under − 300, − 500 and

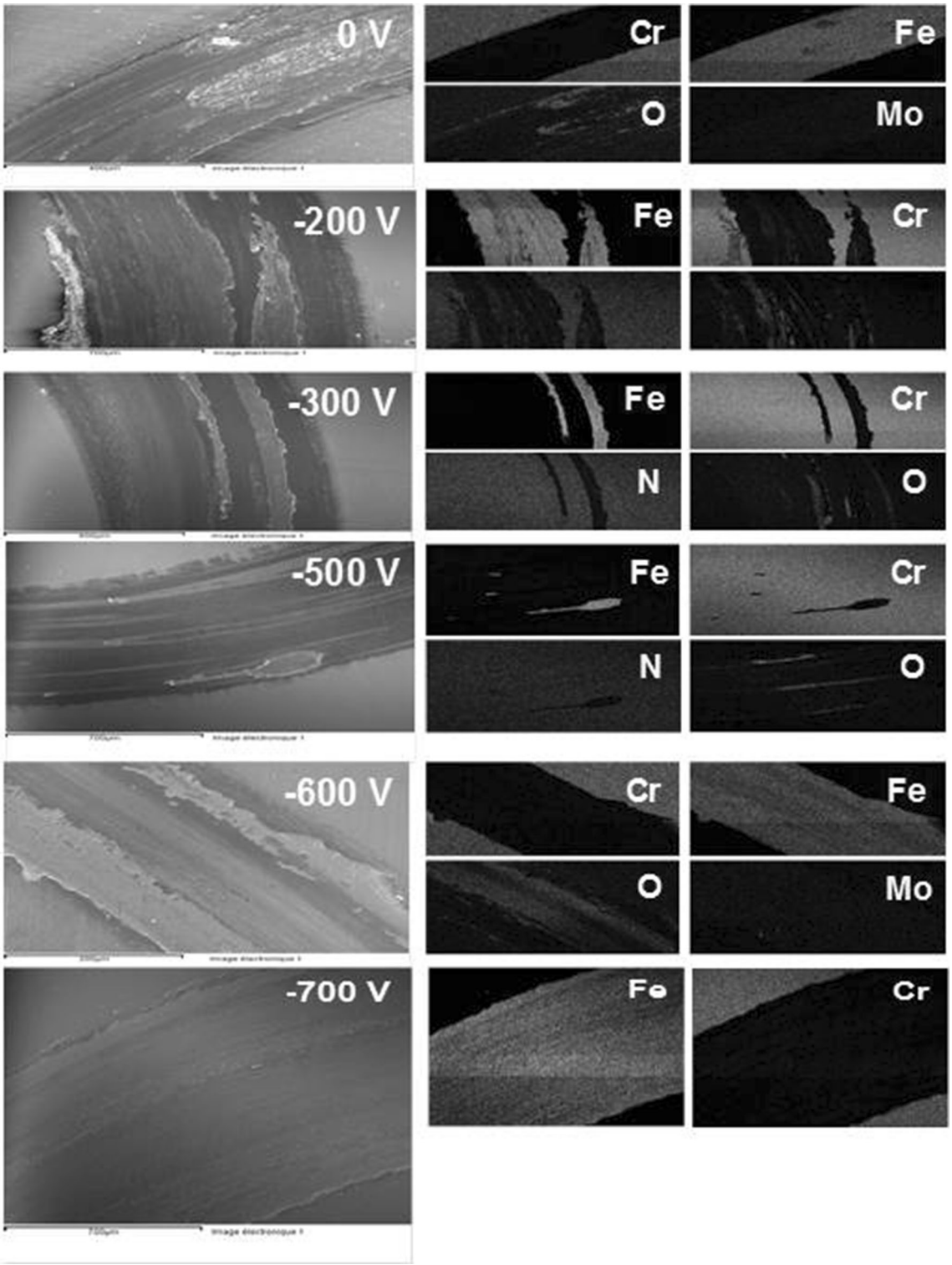

Fig. 9 SEM images and chemical elements profiles of the wear track of the CrN coatings after sliding against Al_2O_3 balls

− 600 V. Nevertheless, the hardness and Young modulus decrease for a substrate bias voltage of − 600 and − 700 V. This can be due to the break of bond resultant with the higher energetic ion bombardment. This can be also related to the weak CrN (111) diffraction peak as shown in Fig. 6, revealing a low coating crystallinity. Also, the decrease in the hardness of coatings is attributed to the stress relaxation and the grain growth (Ref 46). He et al. (Ref 47), who deposited TiN coating by DC reactive magnetron sputtering, explained the decrease in hardness by the increases in defects. Hong et al. (Ref 48) confirmed that hardness was greatly affected by the amounts of coatings defects.

The H^3/E^2 ratio reflects the material ability to resist plastic deformation (Table 3). So, higher the ratio (H^3/E^2) is, higher the resistance to the plastic deformation is. This H^3/E^2 ratio is higher in the case of the CrN coating obtained at − 500 V. One

Table 3 Mechanical properties of the CrN films

Substrate bias voltage, V	Hardness, GPa	Young modulus, GPa	H/E	H^3/E^2	Critical load, N	
					Lc_1	Lc_2
0	14	180	0.077	0.084	5	15
− 200	16	222	0.072	0.083	8	22
− 300	19	235	0.080	0.124	9	35
− 500	22	244	0.090	0.178	12	42
− 600	18	226	0.079	0.114	7.5	25
− 700	15	211	0.071	0.075	7	18

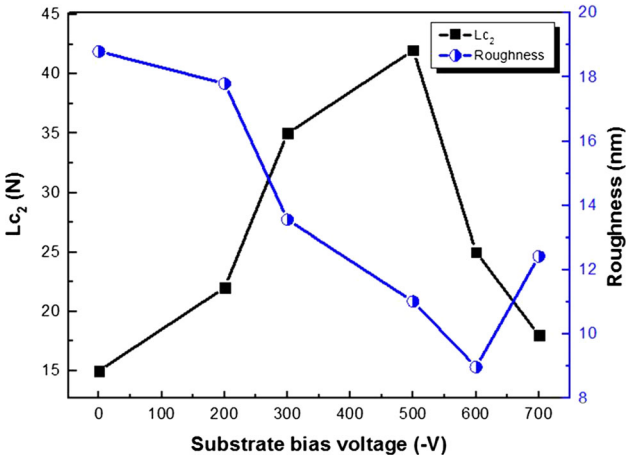

Fig. 10 Critical load Lc_2 and the RMS roughness of the CrN coatings vs. the substrate bias voltage

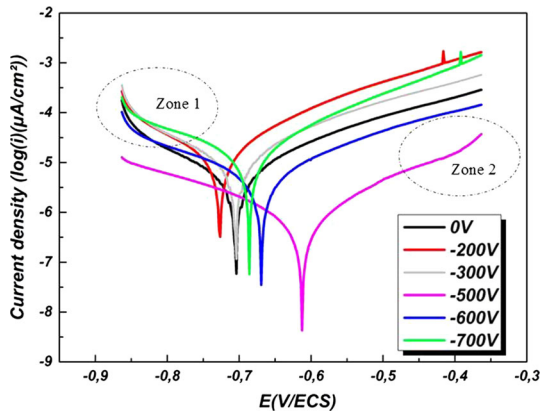

Fig. 11 Electrochemical properties of the CrN coatings as a function of the substrate bias voltage in a 3% NaCl aqueous solution

can conclude that this CrN coating presents the best plastic deformation resistance. This confirms the good behavior of this coating during the friction tests sliding against an alumina ball (Fig. 8 and 9).

Also, the (H/E) ratio which is an indicator of the elastic strain failure has been calculated and is shown in Table 3. This ratio is a valuable parameter for the tribological coating performance. The H/E ratio calculated for unbiased film is about 0.077. With applying a substrate bias voltage, this ratio increases, and it reached 0.09 for a bias of − 500 V. This indicates that the CrN film obtained at − 500 V has the best tribological behavior.

The adhesion properties of CrN coatings are evaluated by scratch test. Lc_1 and Lc_2 represent, respectively, crack initiation resistance and resistance to spallation. As shown in Table 3, it is obvious that the first cohesive failure Lc_1 and the first exposure of substrate Lc_2 of the CrN films are affected by the substrate bias voltage. The Lc_1 critical load increases progressively with the substrate bias voltage up to − 500 V and then it decreases. A similar trend is observed for the Lc_2 critical load. The CrN film obtained without substrate polarization and at − 700 V present the lowest Lc_2 critical loads (15-18 N). This confirms their bad wear behavior and high wear rate (Fig. 8 and 9). By increasing the substrate bias voltage, vertical cracks are created due to the energetic ion bombardment of the CrN films deposited at − 600 and − 700 V (Ref 21, 40). The reduction of the critical load at the highest substrate bias voltages can be attributed to the broken texture of the CrN films. Therefore, the adhesion of the CrN films is also related to their density (Ref 49) and surface roughness. Indeed, critical loads and surface roughness have an inversely proportional behavior (Fig. 10). Higher the RMS is, lower the Lc_2 is. The highest Lc_2 critical load of 42 N is observed for the CrN layer obtained at − 500 V. According to Fig. 8 and 9, this coating was the most wear resistant. We can confirm now that this is probably due to its high adhesion. Besides, as the H/E and Lc_2 curves fit perfectly (Table 3), we can conclude that as expected, the more adherent coating is the one that presents the highest plastic deformation resistance.

3.5 Corrosion

Polarization tests were conducted in a 3% NaCl solution at room temperature (25 °C). The electrochemical properties of the CrN-coated steels samples as a function of the substrate bias voltage are shown in Fig. 11. The CrN coating obtained without substrate bias voltage has a corrosion current of 5.58 μA/cm^2. For a substrate bias voltage of − 200 V the corrosion current increases to 7.63 and to 9.18 μA/cm^2 for a substrate bias voltage of − 300 V. Then, the corrosion current decreases significantly to 0.34 μA/ cm^2 for a substrate bias voltage of − 500 V. It increases again to 2.39 and 6.90 μA/cm^2 for the highest substrate polarizations. The corrosion current generally represents the speed evaluation index of corrosion. Thus, the CrN film obtained at − 500 V provides the best corrosion resistance as it has the lowest corrosion current (Table 4). This good corrosion behavior can be explained by the dense microstructure and low grain size of this CrN coating (Fig. 2 and 4). It has already been shown that a small grain size permits a better corrosion behavior compared

Table 4 Electrochemical properties of CrN coatings as a function of the substrate bias voltage in a 3% NaCl aqueous solution

Substrate bias voltage, V	0	− 200	− 300	− 500	− 600	− 700
E, mV	− 709.3	− 698.7	− 707.6	− 651.2	− 966.8	− 769.7
J, μA/cm^2	5.58	7.63	9.18	0.33	2.38	6.89

with large size-grains (Ref 50). Also, this may be due to the lower number of defects of this coating in comparison with other ones (Fig. 4). Generally, the atoms in areas containing defects have a very high free chemical energy compared with closed areas (Ref 51). These atoms can react with the active particles of the corrosive solution, which produces a surface area of corrosion on the coating. Thereby, one can conclude that the existence of defects reduces the corrosion resistance of the films. Similarly, the good corrosion behavior of the coating obtained at − 500 V may also be due to its better properties such as a low RMS roughness and a high adhesion (Fig. 5 and 10). In general, cracks and grain boundaries provide preferential channels for corrosive agents that can reach the substrate. Finally, the other CrN coatings present a bad corrosion behavior probably because of a low surface density and several defects not neglected as illustrated in Fig. 4 and 5.

Referring to the polarization curve, we note the existence of two zones. In the beginning of the anode area (Zone 1), we observe that the oxygen diffusion level for all films is almost the same except for the CrN film obtained at − 500 V, which is closed to a linear form. Therefore, this film protects the steel substrate surface by the decreasing current. This film acts on the corrosion kinetics or even on the nature of the chemical reactions. Indeed, as this CrN film has fewer pores than the other ones, their closure with the oxide will be easier and faster. At the end of the cathodic area (Zone 2), we observe the existence of a potential for pitting of the CrN film obtained at − 500 V. This phenomenon results in the breaking of the oxide film by Cl^- ions. In addition, this phenomenon can be created by the presence of inclusions on the surface. Finally, one can conclude that the polarization curve confirms that the CrN layer obtained at − 500 V has the best corrosion resistance.

4. Conclusions

CrN properties such as microstructure, tribological and corrosion behavior as a function of the substrate bias voltage were studied during this present work. The conclusions are as follows:

- The deposition rate increased to a maximum for the CrN layer obtained with a substrate bias voltage of − 200 V and then it decreased. The deposition rate increase is attributed to a high energetic ion bombardment while its decrease is due to the increase in etching rate.
- The substrate bias voltage influenced the grains size that varied from 21 to 29 nm. The CrN film obtained at − 200 V has the bigger grain size probably because of the high adatoms mobility and the migration of particles to grains boundaries.
- Cross-sectional SEM images showed that the CrN layers obtained with a substrate polarization have a dense columnar structure.
- The CrN layer obtained with a substrate bias voltage of − 500 V presented the best adhesion, the best plastic deformation resistance, the best friction wear resistance, the highest hardness and Young modulus, the lowest COF, the lowest grain size, a low RMS, the highest tensile stresses and the best corrosion resistance. One can conclude that this CrN layer would be a very good protective material for mechanical applications such as machining process under severe atmosphere.

Acknowledgments

The authors would like to thank the Regional Council of Burgundy for its financial support, Dr. Philippe JACQUET for the XRD analyses and Mr. Denis LAGADRILLERE for the SEM observations and EDS microanalyses.

References

1. A. Kusiak, J. Battaglia, and R. Marchal, Influence of CrN Coating in Wood Machining from Heat Flux Estimation in the Tool, *Int. J. Therm. Sci.*, 2005, **44**, p 289–301
2. H.Y. Lee, J.G. Han, S.H. Baeg, and S.H. Yang, Structure and Properties of WC-CrAlN Superlattice Films by Cathodic Arc Ion Plating Process, *Thin Solid Films*, 2002, **421**, p 414–420
3. P. Gogolewski, J. Klimke, A. Krell, and P. Beer, Al_2O_3 Tools Towards Effective Machining of Wood-Based Materials, *J. Mater. Proc. Technol.*, 2009, **209**, p 2231–2236
4. T. Polcar, N.M.G. Parreira, and R. Novák, Friction and Wear Behaviour of CrN Coating at Temperatures up to 500 °C, *Surf. Coat. Technol.*, 2007, **201**, p 5228–5235
5. S. Inoue, F. Okada, and K. Koterazawa, CrN Films Deposited by RF Reactive Sputtering Using a Plasma Emission Monitoring Control, *Vacuum*, 2002, **66**, p 227–231
6. T. Hurkmans, D.B. Lewis, J.S. Brooks, and W.-D. Munz, Chromium Nitride Coatings Grown by Unbalanced Magnetron (UBM) and Combined Arc/Unbalanced Magnetron (ABSTM) Deposition Techniques, *Surf. Coat. Technol.*, 1996, **87**, p 192–199
7. J.J. Lin, N. Zhang, W.D. Sproul, and J.J. Moore, A Comparison of the Oxidation Behavior of CrN Films Deposited Using Continuous DC, Pulsed DC and Modulated Pulsed Power Magnetron Sputtering, *Surf. Coat. Technol.*, 2012, **206**, p 3283–3290
8. J. Lin, J.J. Moore, W.D. Sproul, B. Mishra, Z. Wu, and J. Wang, The Structure and Properties of Chromium Nitride Coatings Deposited Using DC, Pulsed DC and Modulated Pulse Power Magnetron Sputtering, *Surf. Coat. Technol.*, 2010, **204**, p 2230–2239
9. Z.B. Zhao, Z.U. Rek, S.M. Yalisove, and J.C. Bilello, Phase Formation and Structure of Magnetron Sputtered Chromium Nitride Films: In Situ and Ex Situ Studies, *Surf. Coat. Technol.*, 2004, **185**, p 329–339
10. E. Broszeit, C. Friedrich, and G. Berg, Deposition, Properties and Applications of PVD CrN Coatings, *Surf. Coat. Technol.*, 1999, **115**, p 9–16
11. C. Nouveau, E. Jorand, C. Decès-Petit, C. Labidi, and M. Djouadi, Influence of Carbide Substrates on Tribological Properties of Chromium and Chromium Nitride Coatings: Application to Wood Machining, *Wear*, 2005, **258**, p 157–165

12. M. Oden, C. Ericsson, G. Hakansson, and H. Ljungcrantz, Microstructure and Mechanical Behavior of Arc-Evaporated Cr-N Coatings, *Surf. Coat. Technol.*, 1999, **114**, p 39–51
13. X.S. Wan, S.S. Zhao, Y. Yang, J. Gong, and C. Sun, Effects of Nitrogen Pressure and Pulse Bias Voltage on the Properties of Cr-N Coatings Deposited by Arc Ion Plating, *Surf. Coat. Technol.*, 2010, **204**, p 1800–1810
14. B. Warcholinski and A. Gilewicz, Effect of Substrate Bias Voltage on the Properties of CrCN and CrN Coatings Deposited by Cathodic Arc Evaporation, *Vacuum*, 2013, **90**, p 145–150
15. K. Valleti, A. Jyothirmayi, M. Ramakrishna, and S.V. Joshi, Influence of Substrate Temperature and Bias Voltage on Properties of Chromium Nitride Thin Films Deposited by Cylindrical Cathodic Arc Deposition, *J. Vac. Sci. Technol., A*, 2011, **29**(5), p 051515
16. C. Luo, H. Zhang, J. Shang, and S. Duo, Effect of Bias Voltage on Microstructure and Mechanical Properties of CrN Coatings Prepared by Single Target Magnetron Sputtering, *Key Eng. Mater.*, 2016, **697**, p 777–780
17. Q. Kong, L. Ji, H. Li, X. Liu, Y. Wang, J. Chen, and H. Zhou, Influence of Substrate Bias Voltage on the Microstructure and Residual Stress of CrN Films Deposited by Medium Frequency Magnetron Sputtering, *Mater. Sci. Eng.*, 2011, **176**, p 850–854
18. E. Eser, R.E. Ogilvie, and K.A. Taylor, The Effect of Bias on DC and RF Sputtering WCCo Coating, *Thin Solid Films*, 1980, **67**, p 265–277
19. H.-W. Chang, P.-K. Huang, J.-W. Yeh, A. Davison, C.-H. Tsau, and C.-C. Yangh, Influence of Substrate Bias, Deposition Temperature and Post-deposition Annealing on the Structure and Properties of Multi-principal-component (AlCrMoSiTi)N Coatings, *Surf. Coat. Technol.*, 2008, **202**, p 3360–3366
20. C. Chang and C. Huang, Effect of Bias Voltage on Microstructure, Mechanical and Wear Properties of AlSiN Coatings Deposited by Cathodic Arc Evaporation, *Thin Solid Films*, 2011, **519**, p 4923–4927
21. Z. Wang, D. Zhang, P. Ke, X. Liu, and A. Wang, Influence of Substrate Negative Bias on Structure and Properties of TiN Coatings Prepared by Hybrid HIPIMS Method, *J. Mater. Sci. Technol.*, 2015, **31**, p 37–42
22. M.R. Ardigo, M. Ahmed, and A. Besnard, Stoney Formula: Investigation of Curvature Measurements by Optical Profilometer, *Adv. Mater. Res.*, 2014, **996**, p 361–366
23. K. Rahmoun, A. Iost, V. Keryvin, G. Guillemot, and N.E.C. Sari, A Multilayer Model for Describing Hardness Variations of Aged Porous Silicon Low-Dielectric-Constant Thin Films, *Thin Solid Films*, 2009, **518**, p 213–221
24. V.D. Ovcharenko, A.S. Kuprin, G.N. Tolmachova, I.V. Kolodiy, A. Gilewicz, O. Lupicka, J. Rochowicz, and B. Warcholinski, Deposition of Chromium Nitride Coatings Using Vacuum Arc Plasma in Increased Negative Substrate Bias Voltage, *Vaccum*, 2015, **117**, p 27–34
25. D. Tsai, S. Liang, Z. Chang, T. Lin, M. Shiao, and F. Shieu, Effects of Substrate Bias on Structure and Mechanical Properties of (TiVCrZrHf)N Coatings, *Surf. Coat. Technol.*, 2012, **207**, p 293–299
26. A.J. Detor, A.M. Hodge, E. Chason, Y. Wang, H. Xu, M. Conyers, A. Nikroo, and A. Hamza, Stress and Microstructure Evolution in Thick Sputtered Films, *Acta Mater.*, 2009, **57**, p 2055–2065
27. Y. Lv, L. Ji, X. Liu, H. Li, H. Zhou, and J. Chen, Influence of Substrate Bias Voltage on Structure and Properties of the CrAlN Films Deposited by Unbalanced Magnetron Sputtering, *Appl. Surf. Sci.*, 2012, **258**, p 3864–3870
28. Q. Wang, S. Kwon, and K. Kim, Formation of Nanocrystalline Microstructure in Arc Ion Plated CrN Films, *Trans. Nonferr. Met. Soc. China*, 2011, **21**, p 73–77
29. C. Hsu, K. Chen, Z. Lin, C. Su, and C. Lin, Bias Effects on the Tribological Behavior of Cathodic Arc Evaporated CrTiAlN Coatings on AISI, 304 Stainless Steel, *Thin Solid Films*, 2010, **518**, p 3825–3829
30. J.J. Olaya, S.E. Rodil, S. Muhl, and E. Sanchez, Comparative Study of Chromium Nitride Coatings Deposited by Unbalanced and Balanced Magnetron Sputtering, *Thin Solid Films*, 2005, **474**, p 119–126
31. C.V. Thompson and R. Carel, Stress and Grain Growth in Thin Films, *J. Mech. Phys. Solids*, 1996, **44**, p 657–673
32. Q. Ma, L. Li, Y. Xu, J. Gu, L. Wang, and Y. Xu, Effect of Bias Voltage on TiAlSiN Nanocomposite Coatings Deposited by HiPIMS, *Appl. Surf. Sci.*, 2017, **392**, p 826–833
33. E. Forniés, R.E. Galindo, O. Sánchez, and J.M. Albella, Growth of CrN_x Films by DC Reactive Magnetron Sputtering at Constant N_2/Ar Gas Flow, *Surf. Coat. Technol.*, 2006, **200**, p 6047–6053
34. G.P. Zhang, G.J. Gao, X.Q. Wang, G.H. Lv, L. Zhou, H. Chen, H. Pang, and S.Z. Yang, Influence of Pulsed Substrate Bias on the Structure and Properties of Ti-Al-N Films Deposited by Cathodic Vacuum Arc, *Appl. Surf. Sci.*, 2012, **258**, p 7274–7279
35. T. Lin, L. Wang, X. Wang, Y. Zhang, and Y. Yu, Influence of Bias Voltage on Microstructure and Phase Transition Properties of VO_2 Thin Film Synthesized by HiPIMS, *Surf. Coat. Technol.*, 2016, **305**, p 110–115
36. S.G. Wang, E.K. Tian, and C.W. Lung, Surface Energy of Arbitrary Crystal Plane of bcc and fcc Metals, *J. Phys. Chem. Solids*, 2000, **61**, p 1295–1300
37. Y.X. Wang, S. Zhang, J.-W. Lee, W.S. Lew, and B. Li, Influence of Bias Voltage on the Hardness and Toughness of CrAlN Coatings via Magnetron Sputtering, *Surf. Coat. Technol.*, 2012, **206**, p 5103–5107
38. J. Pelleg, L.Z. Zevin, and S. Lungo, Reactive-Sputter-Deposited TiN Films on Glass Substrates, *Thin Solid Films*, 1991, **197**, p 117–128
39. F. Lomello, F. Sanchette, F. Schuster, M. Tabarant, and A. Billard, Influence of Bias Voltage on Properties of AlCrN Coatings Prepared by Cathodic Arc Deposition, *Surf. Coat. Technol.*, 2013, **24**, p 77–81
40. F. Zhou, K. Chen, M. Wang, X. Xu, H. Meng, M. Yu, and Z. Dai, Friction and Wear Properties of CrN Coatings Sliding Against Si_3N_4 Balls in Water and Air, *Wear*, 2008, **65**, p 1029–1037
41. Y.N. Kok, P.E. Hovsepian, Q. Luo, D.B. Lewis, J.G. Wen, and I. Petrov, Influence of the Bias Voltage on the Structure and the Tribological Performance of Nanoscale Multilayer C/Cr PVD Coatings, *Thin Solid Films*, 2005, **475**, p 219–226
42. J. Romero, M.A. Gómez, J. Esteve, F. Montalà, L. Carreras, M. Grifol, and A. Lousa, CrAlN Coatings Deposited by Cathodic Arc Evaporation at Different Substrate Bias, *Thin Solid Films*, 2006, **515**, p 113–117
43. B. Biswas, Y. Purandare, I. Khan, and P.E. Hovsepian, Effect of Substrate Bias Voltage on Defect Generation and Their Influence on Corrosion and Tribological Properties of HIPIMS Deposited CrN/NbN Coatings, *Surf. Coat. Technol.*, 2018, **344**, p 383–393
44. J.C. Ding, Q.M. Wang, Z.R. Liu, S. Jeong, T.F. Zhang, and K.H. Kim, Influence of Bias Voltage on the Microstructure, Mechanical and Corrosion Properties of AlSiN Films Deposited by HiPIMS Technique, *J. Alloys Compd.*, 2019, **772**, p 112–121
45. L. Bait, L. Azzouz, N. Madaoui, and N. Saoula, Influence of Substrate Bias Voltage on the Properties Of TiO_2 Deposited by Radio-Frequency Magnetron Sputtering on 304L for Biomaterials Applications, *Appl. Surf. Sci.*, 2017, **395**, p 72–77
46. D. Jianxin, W. Fengfang, L. Yunsong, X. Youqiang, and L. Shipeng, Erosion Wear of CrN, TiN, CrAlN, and TiAlN PVD Nitride Coatings, *Int. J. Refract. Met. Hard Mater.*, 2012, **35**, p 10–16
47. C. He, J. Zhang, G. Ma, Z. Du, J. Wang, and D. Zhao, Influence of Bias Voltage on Structure, Mechanical and Corrosion Properties of Reactively Sputtered Nanocrystalline TiN Films, *J. Iron Steel Res. Inter.*, 2017, **24**, p 1223–1230
48. S.G. Hong, S.H. Kwon, S.W. Kang, and K.H. Kim, Influence of Substrate Bias Voltage on Structure and Properties of Cr-Mo-Si-N Coatings Prepared by a Hybrid Coating System, *Surf. Coat. Technol.*, 2008, **203**, p 624–627
49. N. Liu, L. Dong, X. Li, D. Li, R. Wan, and H. Gu, Controllable Substrate Bias Voltages Effectively Tailoring Nanocomposite Nb-B-Al-O Film Properties, *J. Alloys Compd.*, 2015, **636**, p 363–367
50. H. Hsueh, W. Shen, M. Tsai, and J. Yeh, Effect of Nitrogen Content and Substrate Bias on Mechanical and Corrosion Properties of High-Entropy Films $(AlCrSiTiZr)_{100-x}N_x$, *Surf. Coat. Technol.*, 2012, **206**, p 4106–4112
51. M. Flores, L. Huerta, R. Escamilla, E. Andrade, and S. Muhl, Effect of Substrate Bias Voltage on Corrosion of TiN/Ti Multilayers Deposited by Magnetron Sputtering, *Appl. Surf. Sci.*, 2007, **253**, p 7192–7196